JOURNAL OF Materials CHEMISTRY

Racemic and enantiomerically pure phenyl α-nitronyl nitroxide radicals: influence of chirality on solution and solid state properties†

Maria Minguet,[a] David B. Amabilino,*[a] José Vidal-Gancedo,[a] Klaus Wurst[b] and Jaume Veciana*[a]

[a]*Institut de Ciència de Materials de Barcelona (CSIC), Campus Universitari, 08193 Bellaterra, Catalonia, Spain. Tel: 34 93 580 1853; Fax: 34 93 580 5729; E-mail: vecianaj@icmab.es; amabilino@icmab.es*

[b]*Institut für Allgemeine Anorganische und Theoretische Chemie, Universität Innsbrück, A-6020, Innrain 52a, Austria*

Received 13th July 2001, Accepted 12th November 2001
First published as an Advance Article on the web 15th January 2002

Two chiral phenyl α-nitronyl nitroxides‡ substituted in the aromatic ring with a lactate moiety have been prepared in their enantiopure and racemic forms. The X-ray crystal structures of the racemic methyl ester and both the racemic and enantiopure carboxylic acid have been solved. The ester forms chains of molecules linked by weak hydrogen bonds, while the racemic acid also forms chains, but linked by strong hydrogen bonds between the acid OH group and one of the nitroxide oxygen atoms. In stark contrast, the racemic acid forms cyclic hydrogen bonded dimers by virtue of the same interaction. In addition, these dimers are observed in solution state for both enantiopure and racemic acids as witnessed by EPR spectroscopy. The ground state of the cyclic aggregates appears to be a triplet with a very weak magnetic interaction. Circular dichroism spectroscopy of the chiral compound reveals additional evidence for dimer formation, while LDI–TOF mass spectrometry indicates the presence of chains in amorphous films of the compounds. Magnetic susceptibility measurements of the solids reveal antiferromagnetic interactions in all cases: in the racemic ester and enantiopure acid they are weak, while in the racemic acid they are strong as a result interactions between cyclic dimers.

Introduction

While the use of the influence of chirality on the properties of several types of molecular materials is well established,[1,2] the consequences for magnetic materials are less well known, though the potential for magneto-optical phenomena is a particularly interesting area.[3] Some interesting examples of chiral coordination compounds incorporating paramagnetic metal ions have been reported,[4] and chiral organic radicals have been prepared.[5] Our interest lies in this second group of materials, specifically chiral phenyl α-nitronyl nitroxide‡ radicals.[6] These compounds, part of the extensive family of α-nitronyl nitroxides[7] so popular among those studying molecular magnetism,[8] are prepared with the aim of establishing some of the effects of stereochemistry in molecular magnetic materials. Here we report the solution (EPR and circular dichroism) and solid state (structure and magnetic susceptibility) characteristics of the radicals (*R*)-**4MLNN**, (*RS*)-**4MLNN**, (*R*)-**4LNN**, and (*RS*)-**4LNN** (Scheme 1).

Results and discussion

Synthesis

The radicals were synthesised (Scheme 1) by the Mitsunobu reaction[9] of 4-hydroxybenzaldehyde with (*S*)- or (*RS*)-methyl lactate followed by condensation of the resulting chiral aldehydes **1** with 2,3-bis(hydroxylammonio)-2,3-dimethylbutane sulfate[10] (**2**) and oxidation of the resulting products **3** with sodium periodate (according to Ullman's procedure[11]) to give

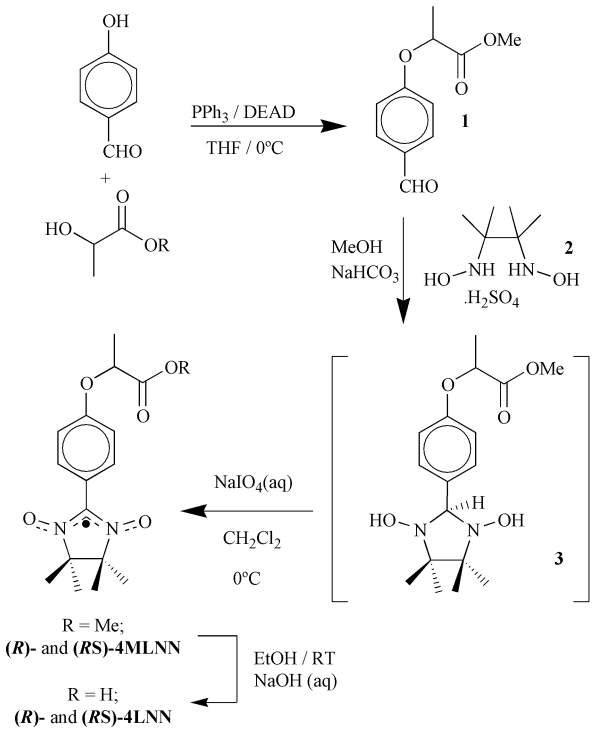

Scheme 1

†Electronic supplementary information (ESI) available: figures showing alternative views of the crystal structures and the shortest distances between SOMOs in the crystals. See http://www.rsc.org/suppdata/jm/b1/b106239p/

‡The IUPAC name for these phenyl α-nitronyl nitroxides is 2-phenyl-4,5-dihydro-4,4,5,5-tetramethyl-3-oxido-1*H*-imidazol-3-ium-1-oxyl.

 DOI: 10.1039/b106239p

the esters (*R*)-**4MLNN** and (*RS*)-**4MLNN**. These compounds were saponified with sodium hydroxide in aqueous ethanol to give the corresponding carboxylic acids (*R*)-**4LNN** and (*RS*)-**4LNN**.

Solid state structures

The X-ray crystal structure of (*RS*)-**4MLNN** (space group $P2_1/c$, Table 1) reveals molecules with a pseudo-eclipsed conformation,[12] in which the torsion angles (i) between the phenyl and imidazolyl rings (A_{PNN}) and (ii) of the NCCN unit in the imidazolyl ring (T_{IM}) are opposite giving the molecule a relatively planar general form when compared with the alternative pseudo-*anti* conformation.[12] The *R* enantiomer in the racemic crystals has *PM* chirality and the *S* has *MP*, the torsion angles A_{PNN} and T_{IM} being 13.6 and 19.6° respectively (Fig. 1). The molecules pack together in the form of homochiral chains which run along the crystallographic *b* axis (Fig. 2) in which the molecules are linked through three [C_{sp^3}–H···O] hydrogen bonds.[12–14] Two act between methyl groups attached to the imidazolyl ring of one molecule and one of the NO groups of the next, and the other to the carbonyl group of the first molecule from a different hydrogen atom in the related methyl group of the second molecule (See Table 2 for distances and angles). These undulating chains come together in an antiparallel fashion to give a three dimensional structure without the formation of other significant non-covalent interactions. Despite numerous attempts, (*R*)-**4MLNN**, the enantiopure form of this compound, could not be crystallised to give X-ray quality crystals, preventing a comparison of the conformations in the two modifications.

The enantiopure lactic acid-derived radical (*R*)-**4LNN** crystallises in the $P2_12_12_1$ space group with just one molecule in the asymmetric unit which has a pseudo-eclipsed *PM* conformation[15] (Fig. 3), the same gross form as the corresponding enantiomer in crystals of (*RS*)-**4MLNN**. Unusual in the molecule is the difference between the two N–O bond lengths (1.276(4) and 1.301(4) Å), an effect which is caused by the formation of a strong intermolecular hydrogen bond between the acidic hydrogen atom of one molecule and the oxygen atom associated with the longer N–O group of a neighbouring one. This hydrogen bond is aided by the existence of two hydrogen bonds formed by the carbonyl group and hydrogen atoms of two different methyl groups attached to the imidazolyl ring (Table 2), and leads to the formation of non-covalent chains which run along the crystallographic *c* axis. These chains aggregate along the *b* axis direction in an antiparallel fashion by virtue of a [C_{sp^2}–H···O] hydrogen bond

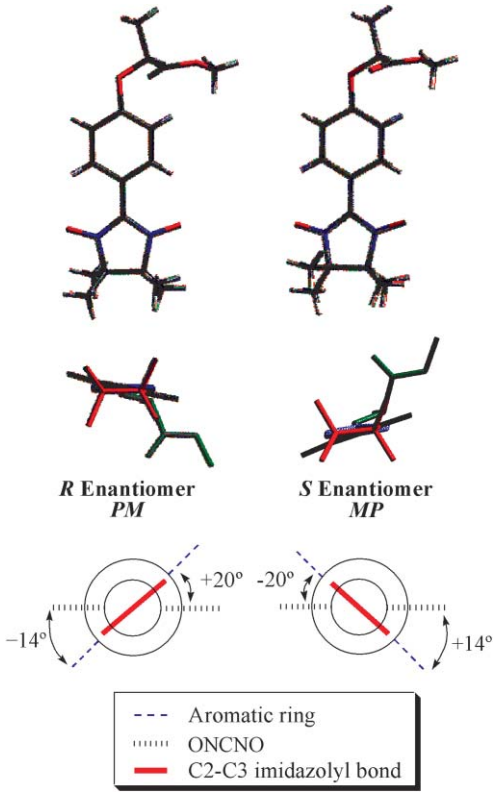

Fig. 1 Views of the enantiomeric molecules of **4MLNN** in the crystal structure of the racemate and a representation of the molecule as viewed down the long axis from the imidazolyl end of the molecule, showing the pseudo-eclipsed arrangement of the rings.

Table 1 Crystallographic data for (*RS*)-**4MLNN**, (*RS*)-**4LNN** and (*R*)-**4LNN**

Compound	(*RS*)-**4MLNN**	(*RS*)-**4LNN**	(*R*)-**4LNN**
Formula	$C_{17}H_{23}N_2O_5$	$C_{16}H_{21}N_2O_5$	$C_{16}H_{21}N_2O_5$
M	335.37	321.35	321.35
Colour, habit	Dark blue prisms	Dark blue prisms	Dark blue plates
Crystal dimensions/mm	0.7 × 0.4 × 0.25	0.2 × 0.2 × 0.15	0.5 × 0.3 × 0.045
T/K	218(2)	218(2)	218(2)
Radiation (λ/Å)	MoKα (0.71073)	MoKα (0.71073)	MoKα (0.71073)
System	Monoclinic	Triclinic	Orthorhombic
Space group	$P2_1/c$	$P\bar{1}$	$P2_12_12_1$
a/Å	8.307(3)	8.5129(5)	6.910(2)
B/Å	10.366(3)	9.4113(7)	11.910(3)
c/Å	20.439(4)	10.4820(8)	19.481(5)
α/°		85.847(3)	90
β/°	97.11(2)	76.415(4)	90
γ/°		79.503(4)	90
V/Å^3	1746.5(9)	802.25(10)	1603.2(7)
Z	4	2	4
D_c/g/cm^3	1.275	1.330	1.331
F(000)	716	342	684
θ range/°	2.8–23.5	2.0–23.5	2.7–20.5
Measured reflections	2564	2354	1207
Observed reflections, ($I > 2\sigma(I)$)	2098	1957	1048
Parameters	224	217	213
Restrictions	0	0	0
R ($I > 2\sigma(I)$)	0.0445	0.0430	0.0322
wR_2 ($I > 2\sigma(I)$)	0.1100	0.1045	0.0730
R (all data)	0.0570	0.0542	0.0413
wR_2 (all data)	0.1161	0.1099	0.0767

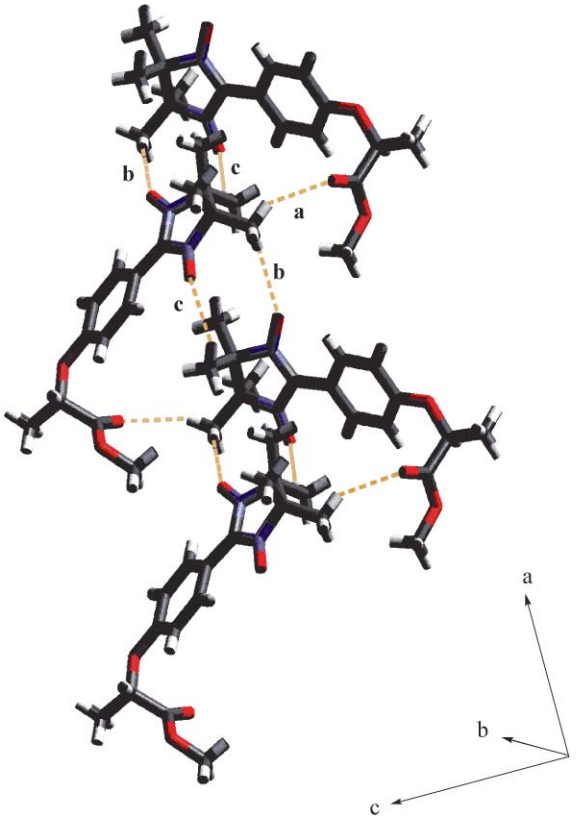

Fig. 2 The hydrogen bonded chains formed in the crystal structure of (*RS*)-**4MLNN**. Hydrogen bonds: a) $C_{Me}22$–H···O4=C; b) $C_{Me}22$–H···O2–N; c) $C_{Me}32$–H···O1–N.

between the "free' N–O group and a hydrogen at the 3-position of the aromatic ring in a neighbouring chain as well as a [C_{sp^3}–H···O] hydrogen bond from one of the imidazolyl groups to the ether oxygen atom in every second molecule of the chain (Table 2). These aggregated chains form highly

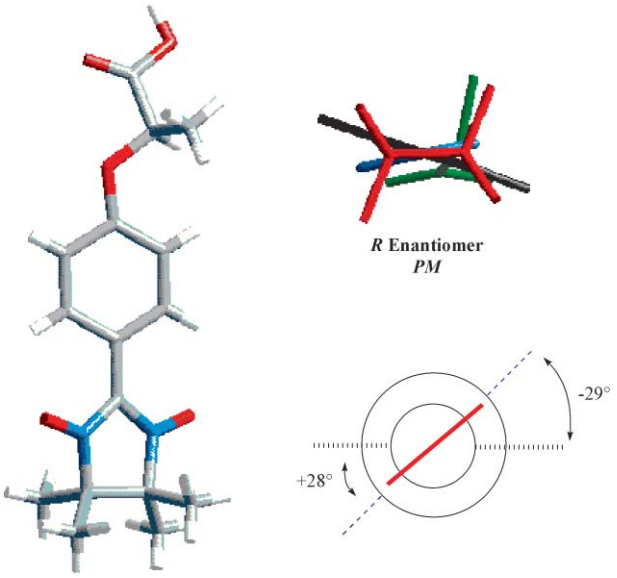

Fig. 3 Views of (*R*)-**4LNN** in its crystal structure and a representation of the molecule as viewed down the long axis (see Fig. 1 for key).

corrugated sheets that pile up along the *a* axis (Fig. 4). The chains stack in a parallel manner with the formation of several [C_{sp^3}–H···O] hydrogen bonds (Table 2) and a [C_{sp^3}–H···π] interaction of the methyl group attached to the stereogenic centre and the benzene ring (shortest H···C distance 2.893 Å, C···C distance 3.369 Å) (Fig. 4).

The racemate of the lactic acid-derived radical **4LNN** crystallises in the triclinic space group $P\bar{1}$. The centrosymmetrically-related *R* and *S* enantiomers have pseudo-eclipsed *PM* and *MP* conformations, respectively (Fig. 5). Therefore, once again the *R* enantiomer in this racemate has the same gross conformation of the two ring system (angle A_{PNN}) as in the other compounds reported here. The density of the racemate is practically the same as that of the enantiopure compound, in

Table 2 Hydrogen bond distances and geometries found in crystals of (*RS*)-**4MLNN**, (*RS*)-**4LNN** and (*R*)-**4LNN**

Radical	H-bond[a]	[H···O] distance/Å	[X–H–O] angle/°	[X–H–O] distance/Å
(*RS*)-**4MLNN**	$C_{Me}22$–H···O2–N	2.73	163	3.671(3)[i]
	$C_{Me}32$–H···O1–N	2.86	159	3.779(4)[j]
	$C_{Me}22$–H···O4=C	2.63	143	3.452(3)[j]
(*RS*)-**4LNN**	O3–H···O1–N[b]	1.73	168	2.664(2)[k]
	$^{Im}C_{Me}22$–H···O2–N[c]	2.59	164	3.532(3)[l]
	$C_{meta}6$-H···O2–N[d]	2.53	172	3.470(3)[m]
	C*10–H···O2–N[d]	2.69	154	3.606(3)[m]
	$C_{ortho}9$–H···O3(H)CO–[d]	2.64	147	3.465(3)[n]
	$^{Im}C_{Me}22$–H···O5–Ph[d]	2.77	143	3.594(3)[o]
	$^{Im}C_{Me}31$–H···O4=C[e]	2.55	159	3.476(3)[p]
	C*$C_{Me}12$–H···O5–Ph[c]	2.73	172	3.696(3)[q]
	C*$C_{Me}12$–H···O1–N[d]	2.79	161	3.723(3)[r]
(*R*)-**4LNN**	O3–H···O2–N[f]	1.63	159	2.619(4)[s]
	$^{Im}C_{Me}22$–H···O4=C[f]	2.67	156	3.579(5)[t]
	$^{Im}C_{Me}32$–H···O4=C[f]	2.74	141	3.546(5)[t]
	C6–H···O2–N[g]	2.33	155	3.210(5)[u]
	$^{Im}C_{Me}22$–H···O5Ph[g]	2.78	177	3.753(5)[u]
	$^{Im}C_{Me}32$–H···O4=C[h]	2.62	153	3.512(5)[v]
	$^{Im}C_{Me}31$–H···O4=C[h]	2.74	148	3.599(5)[v]
	C*$C_{Me}12$–H···O1–N[h]	2.66	144	3.496(5)[w]
	$^{Im}C_{Me}32$–H···O5Ph[h]	2.55	142	3.369(5)[v]

[a]$Im C_{Me}$ signifies the methyl groups attached to the imidazolyl ring, and C*C_{Me} that attached to the stereogenic centre. [b]Intra-dimer hydrogen bonds which link *R* and *S* sheets "face-to-face'. [c]Inter-dimer weak hydrogen bonds (cyclic dimer) which link *R* and *S* sheets "back-to-back'. [d]Intra-homochiral sheet hydrogen bonds. [e]Weak hydrogen bonds between sheets "face-to-face'. [f]Indicates intra-chain hydrogen bond. [g]Indicates intra-sheet hydrogen bond. [h]Indicates intra-stack hydrogen bond. Symmetry operations: [i]$-x, 0.5 + y, 0.5 - z$; [j]$-x, -0.5 + y, 0.5 - z$; [k]$1 - x, 1 - y, 2 - z$; [l]$-x, -y, 2 - z$; [m]$1 + x, y, z$; [n]$-1 + x, y, z$; [o]$x, y, -1 + z$; [p]$-x, 1 - y, 2 - z$; [q]$1 - x, -y, 3 - z$; [r]$x, y, 11 + z$; [s]$-0.5 - x, 1 - y, -0.5 + z$; [t]$-0.5 - x, 1 - y, 0.5 + z$; [u]$-x, 0.5 + y, 0.5 - z$; [v]$0.5 - x, 1 - y, 0.5 + z$; [w]$1 + x, y, z$.

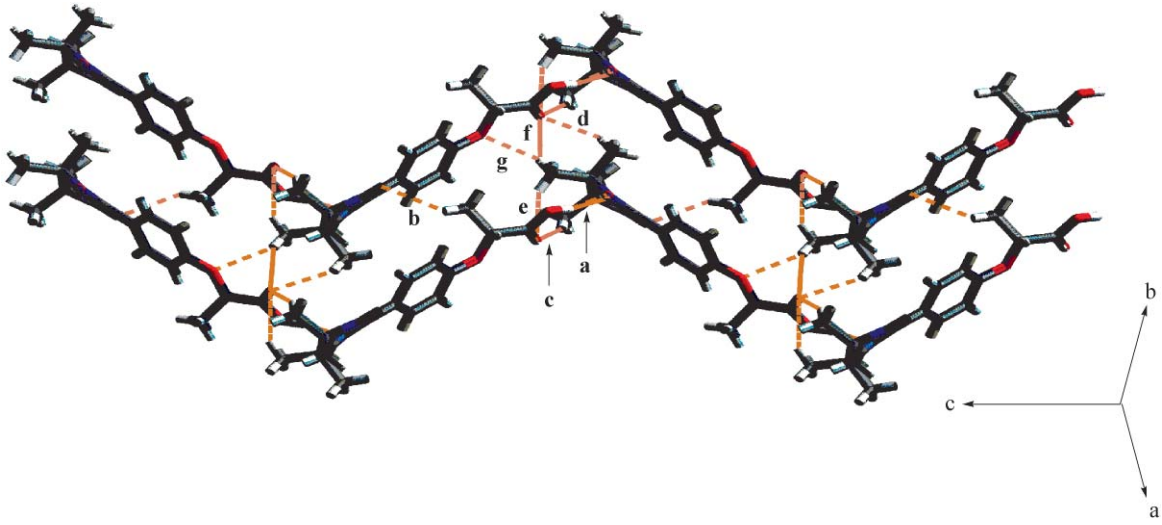

Fig. 4 The parallel-stacked hydrogen bonded chains formed along the *a* axis in the crystal structure of (*R*)-**4LNN**. Hydrogen bonds: a) O3–H···O2–N; b) $C_{Me}12$–H···O1–N; c) $C_{Me}22$–H···O4=C; d) $C_{Me}31$–H···O4=C; e) $C_{Me}32$–H···O4=C; f) $C_{Me}32$–H···O4=C: g) $C_{Me}32$–H···O5Ph.

contradiction to Wallach's rule.[16] In contrast to the enantiopure compound that forms hydrogen bonded chains, (*RS*)-**4LNN** crystallises to form *cyclic dimers* (Fig. 6) held together by the same type of hydrogen bond seen in the former, between the acid group and one of the NO moieties. In this compound, the hydrogen bonds (Table 2) are somewhat longer than in the enantiopure compounds (a fact which might partially explain the contradiction to Wallach's rule), but a significant difference in the N–O bond lengths (1.279(2) and 1.298(2) Å) is observed here too.

The three dimensional structure within the crystals is characterised by the presence of homochiral sheets in the *b* plane in which the molecules are linked together in parallel manner by a series of weak hydrogen bonds of the [C_{sp^3}–H···O] and [C_{sp^2}–H···O] varieties (Fig. 7 and Table 2). These sheets are joined in alternating manner by virtue of the aforementioned cyclic dimers on one side of the sheet, and on the other by the formation of further hydrogen bonds: A cyclic motif between the acid-assembled dimers (the donor and acceptor of the hydrogen atom being one of the methyl groups attached to the imidazolyl ring and the "free' nitroxyl (aminoxyl) group, respectively) and a [C_{sp^3}–H···O] bond between the methyl group attached to the chiral group and the phenoxy oxygen atom.

The observation of a cyclic dimer in the case of the racemic compound and chains for the enantiopure is interesting, and contrasts with the related 3-substituted radicals (*R*)-**3LNN** and (*RS*)-**3LNN**,[6] in which both racemate and enantiopure compound form chains in the crystal. This result indicates, perhaps, that the cyclic dimer of (*RS*)-**4LNN** is a thermodynamically preferred aggregate, but that the kinetics of crystal growth lead to preferential formation of chains in the enantiopure sample. In order to confirm this supposition we performed mass spectral, circular dichroism and electron paramagnetic resonance studies on the radicals.

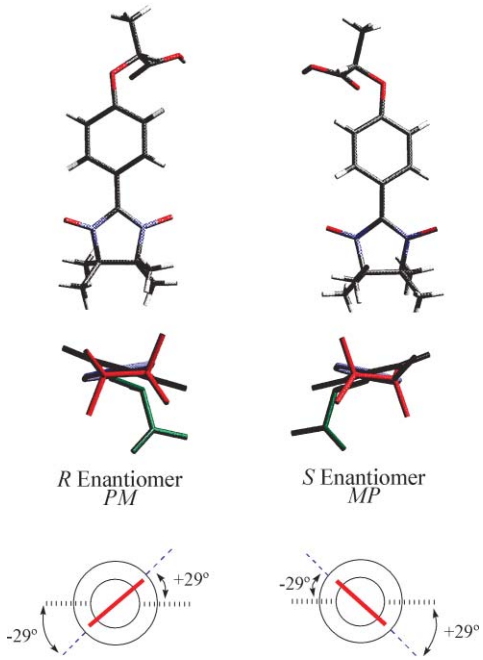

Fig. 5 Views of the enantiomeric molecules of **4LNN** in the crystal structure of the racemate and a representation of the molecules as viewed down their long axis.

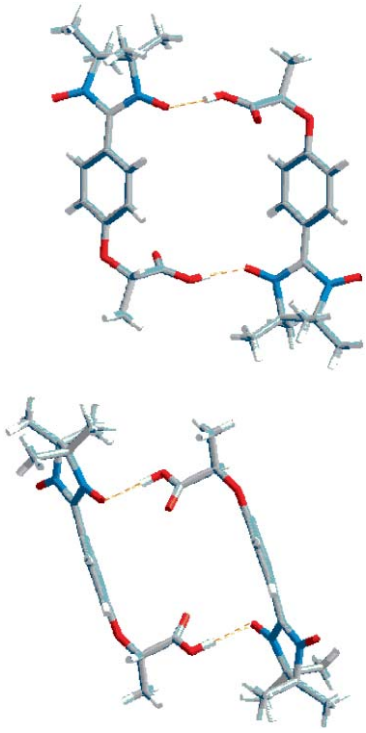

Fig. 6 Two views of the cyclic dimers formed by (*RS*)-**4LNN** in its crystals.

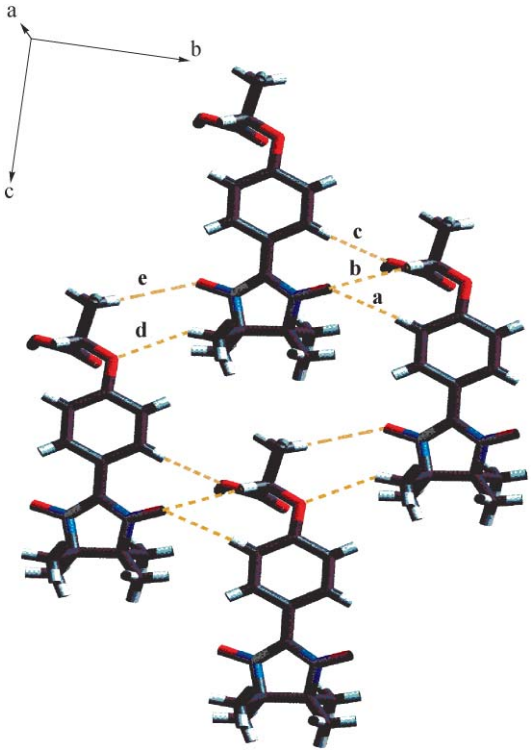

Fig. 7 The homochiral sheets formed by (*RS*)-**4LNN** in its crystals. Hydrogen bonds: a) C6–H···O2–N; b) C10–H···O2–N; c) C9–H···(H)O3–C; d) $C_{Me}22$–H···O5Ph; e) $C_{Me}12$–H···O1–N.

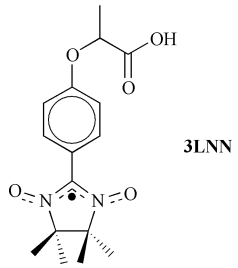

3LNN

Mass spectrometry

The laser desorption ionisation time-of-flight mass spectrum (LDI-TOF MS) of the methyl esters **4MLNN** produced ions with charge to mass ratios consistent with the molecular ions (*m*/*z* 335.2), although the most intense peaks correspond to the loss of oxygen atoms from the compound (Fig. 8), as also witnessed in electron impact mass spectra (EI-MS) of related compounds.[17] No significant signals are observed at higher masses in either technique. In contrast, the spectra of both the enantiomerically pure and racemic modifications of **4LNN** indicate the presence of aggregates in the samples evaporated from dichloromethane solutions. In particular, batches of peaks corresponding to dimeric and trimeric species are observed, in which alkali metal ion adducts and loss of oxygen atoms and carboxylate groups complicate the spectra (Fig. 8). While the spectra provide no quantitative information regarding the linear or cyclic nature of the assemblies, the spectra are indicative of the tendency of the molecules to form aggregates.

Electrospray mass spectrometry (ES-MS) can often provide useful information concerning the formation of "self-assembled' aggregates in solution.[18] ES mass spectra of racemic and enantiopure **4LNN** from toluene solutions of the radicals reveal peaks corresponding to the protonated molecular ion ($[M + H]^+$, 100%) and also to the dimer ($[2M + H]^+$, 20%), giving clear evidence for its formation. An extremely weak ion (<2%) was also observed corresponding to the ($[3M + H]^+$ ion.

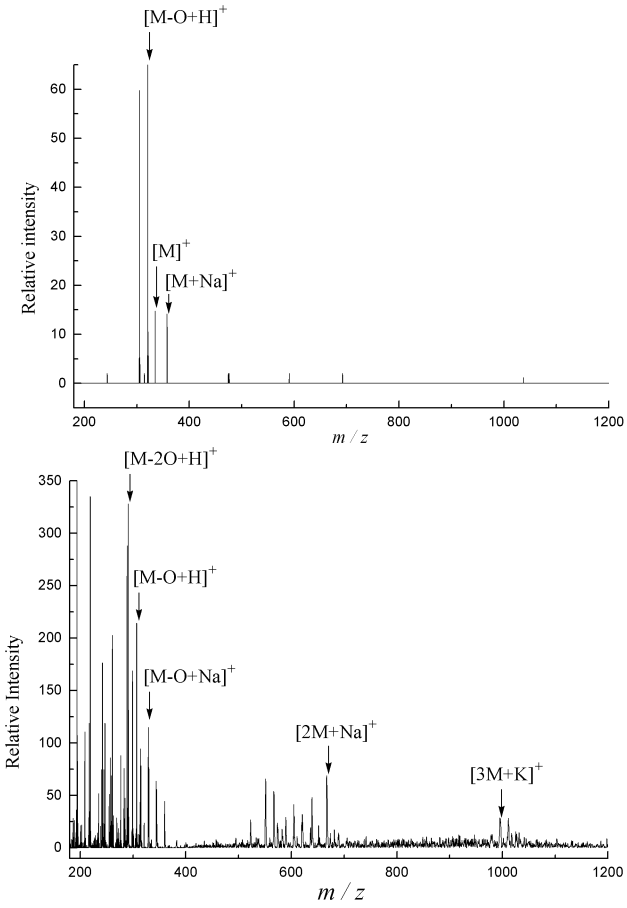

Fig. 8 LDI-TOF mass spectra of (*R*)-**4MLNN** (top) and (*R*)-**4LNN** (bottom).

Circular dichroism

Circular dichroism (CD) can also be a very sensitive tool for the study of aggregation behaviour of chiral molecules.[19] The CD spectrum of the two chiral compounds reported here reveal significant Cotton effects between 200 and 350 nm (Fig. 9), but present no significant optical activity in the visible part of the electromagnetic spectrum (unlike the corresponding 3-substituted analogs[6,20]). This situation probably reflects the large distance and lack of conjugation between the stereogenic centre and the ONCNO unit which is responsible for absorption in this area. The methyl ester (*R*)-**4MLNN** dissolved in dichloromethane presents a weak negative Cotton effect at 365 nm, and a large positive one centred at 275 nm, which are both assigned (on the basis of *ab initio* calculations)[6b] to π→π* transitions, of the ONCNO and phenyl chromophores, respectively. In

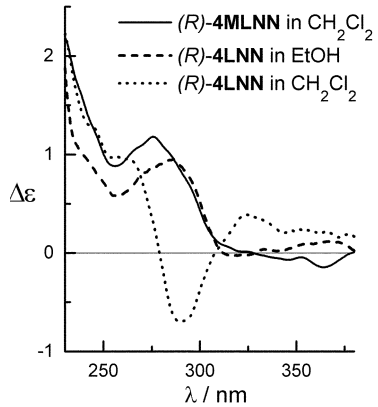

Fig. 9 CD spectra of (*R*)-**4MLNN** in CH_2Cl_2 and (*R*)-**4LNN** in both CH_2Cl_2 and EtOH.

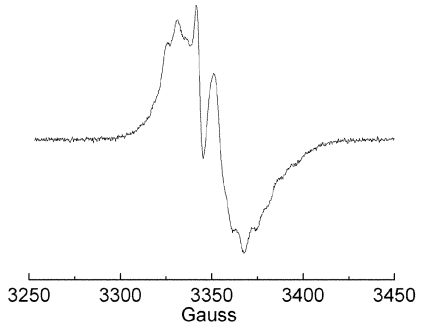

Fig. 10 Full field EPR signal of (*R*)-**4LNN** at 160 K in CH_2Cl_2–toluene 1 : 1.

contrast, in the same solvent the corresponding acid (*R*)-**4LNN** displays a strong negative Cotton effect at 290 nm, and a weak positive one at 325 nm. However, when the same compound is dissolved in ethanol, the spectrum becomes remarkably similar to that of the methyl ester. Therefore, the CD spectrum of the chiral acid in dichloromethane gives strong qualitative evidence for the formation of aggregates in solution, which are destroyed upon addition of a polar and protic solvent, such as ethanol.

Electron paramagnetic resonance

The electron paramagnetic resonance (EPR) spectra of solutions of both the racemic and enantiomerically pure **4LNN** also reveal the presence of aggregates. While dilute solutions of all radicals in dichloromethane–toluene (1 : 1) show the five line pattern with hyperfine splitting patterns typical of the phenyl α-nitronyl nitroxide radicals,[21] concentrated solutions of the acids present strong dipolar signals (Fig. 10) as well as half-field signals at low temperature (Fig. 11), strongly indicative of species with spin greater than ½. No signal was observed at ⅓ field in either case.

The zero field splitting parameters of both the racemic and enantiomerically pure radical **4LNN**, obtained by simulation of the dipolar signal in frozen solution (Fig. 11), are very similar ($D' = 28$ G, $E' = 0$ G). This parameter can be used to calculate the mean effective distance between radical centres (r) using the equation $D' = 27887/r^3$, which is valid for the point dipole approximation. The resulting mean effective distance is approximately 10.0 Å, a value very similar to the distance between the α carbon atoms in the dimer present in the crystals of (*RS*)-**4LNN** (9.67 Å), giving strong support for the same structure in solution for both modifications. Also, it should be pointed out that the EPR spectrum of the corresponding **3LNN** does not indicate the formation of aggregates in solution,[6]

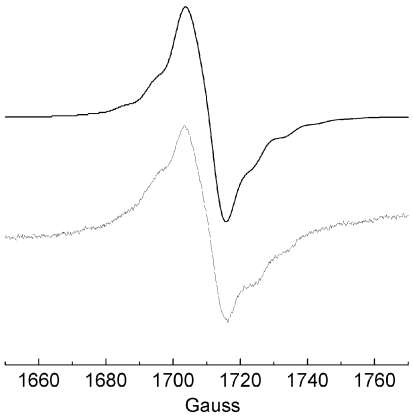

Fig. 11 Half field signal EPR signal of (*R*)-**4LNN** at 4.6 K in CH_2Cl_2–toluene 1 : 1 (bottom) and simulation of the signal with $D' = 28$ G and $E' = 0$ G (top).

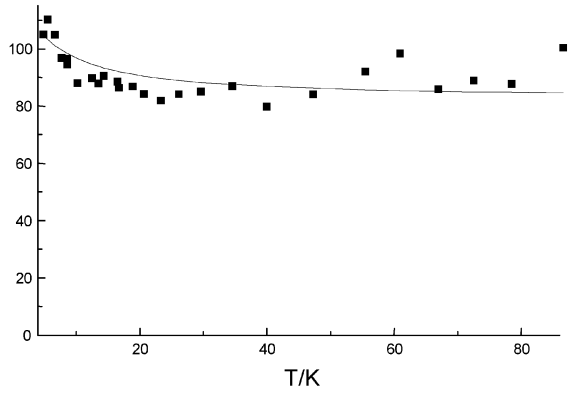

Fig. 12 Temperature dependence of the product of intensity and temperature of the half field EPR signal displayed by (*R*)-**4LNN**.

giving supporting evidence for the notion of a cyclic rather than linear aggregate.

The observation of a half field signal in frozen solutions of the radicals provides the opportunity for studying the magnetic properties of the cyclic dimer by following the intensity of the half-field signal with temperature. In the case that the unpaired electrons in the two radical units of the cyclic dimers behave independently magnetically, the intensity should obey the Curie law, while ferromagnetic or antiferromagnetic interactions between them should lead to positive and negative deviations from it, respectively. The plot of the intensity–temperature product *versus* temperature (Fig. 12) for the half-field signal for (*R*)-**4LNN** shows a gentle rise at very low temperatures indicative of a triplet ground state. Fitting of the curve to the Bleaney–Bowers equation indicates a small ferromagnetic interaction between the spins of $J/k = +4.5$ (± 2 K). While there is much error in the absolute magnitude of this small interaction (arising from difficulty in integration of the EPR spectra), it is clear from the measurements that the triplet is the ground state.

Magnetic properties of the solids

Magnetic susceptibility measurements of ground crystalline samples of the radicals reveal that the exchange interactions (J/k, using the following effective Heisenberg Hamiltonian: $H = -2JS_AS_B$) in all the materials are antiferromagnetic, but by varying degrees (Fig. 13).

The crystals of (*RS*)-**4MLNN** have very weak interactions. In accord with the solid state structure, the susceptibility data were fitted using a one-dimensional antiferromagnetic Heisenberg chain model with molecular field (correlation 99.9%), giving J/k of -0.65 K for the predominant interaction. The weakness of the interaction is not surprising given the remote nature of the singly occupied molecular orbitals (SOMOs)[22]—the nearest NO–ON distance is 4.15 Å—and their quasi-perpendicular orientation (see Supplementary Information†).

The SOMOs in crystals of (*R*)-**4LNN** form chains resulting from contact between α-nitronyl nitroxide moieties in adjacent structural stacks of the molecules. The closest NO–ON distance is relatively large (4.07 Å), and the overlap lies between orthogonal and parallel. Thus, fitting of the magnetic data to a one-dimensional antiferromagnetic Heisenberg chain model (correlation 99.9%) gave the expected weak exchange interaction (J/k of -2.0 K).

In contrast, crystals of (*RS*)-**4LNN** present very strong antiferromagnetic interactions. These interactions surely arise from the close approach between the oxygen atoms bearing the spin in between the non-covalent dimers. The distance between the oxygen atoms is a mere 3.43 Å, and their π-orbital overlap is appreciable (see Supplementary Information†). The magnetic data were fitted to the Bleaney–Bowers equation (correlation 99.7%), giving an exchange coupling (J/k) of

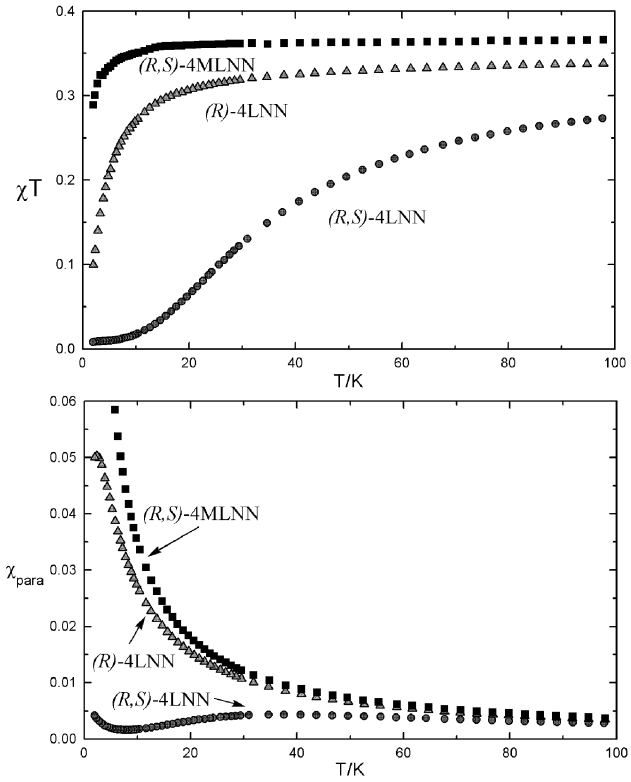

Fig. 13 Temperature dependence of the magnetic susceptibility (χ) (bottom) and magnetic susceptibility (χ) × temperature product (top) of the three crystalline radicals reported here.

−29.6 K. The relatively large magnitude of the antiferromagnetic coupling between dimers makes it practically impossible to observe the very weak ferromagnetic couplings within each dimer which were inferred in the solution state experiments.

Conclusions

We have confirmed that the presence of a stereogenic centre appended to the phenyl α-nitronyl nitroxide radicals leads to the preferential crystallisation of one of the four possible gross conformational isomers for a given enantiomer. In the case of the (*R*)-lactate group attached at the 4-position of the phenyl ring attached to the α-nitronyl nitroxide, the three crystal structures all have molecules of the same gross conformation of the component phenyl and imidazolyl rings, that is the pseudo-eclipsed *PM*.

The modification of the acid derivatives has a very profound effect on the crystal packing and consequently on the magnetic properties of the compounds. While the enantiomerically pure radical **4LNN** forms chains in its crystals and presents very weak antiferromagnetic interactions, the racemic modification crystallises as non-covalent cyclic dimers which interact with each other giving rise to strong antiferromagnetic interactions in spite of the very weak ferromagnetic interaction in operation within dimers.

Cyclic dimers held together by hydrogen bonds between the carboxylic acid function and the nitrone present in the solid state for the racemic compound are also observed in solution for both the racemic and enantiomerically pure modifications of radical **4LNN**. While the dimerisation of the molecules is possible by the carboxylic acid functions in principle,[23] this mode of aggregation has not been observed here, presumably because of the greater strength of the nitrone–carboxylic acid hydrogen bond.[24] The temperature dependence of the half field signal of the aggregate reveals a very small exchange coupling between the free electrons, with the triplet being the ground state.

Experimental

Materials and methods

The following products were purchased commercially (supplier as indicated) and were used without further purification: 4-Hydroxybenzaldehyde (Aldrich, 98%), (*S*)-methyl lactate (Fluka, 97%), (*RS*)-methyl lactate (Fluka, 97%), triphenylphosphine (Merck, 98%), diethyl azodicarboxylate (Aldrich, 85%). 2,3-Bis(hydroxylammonio)-2,3-dimethylbutane sulfate (**2**) was prepared according to a literature method.[10] Thin-layer chromatography (TLC) was performed on aluminium plates coated with Merck Silica gel 60 F_{254}. Developed plates were air-dried and scrutinised under UV lamp. Silica gel 60 (35–70 mesh, SDS) was used for column chromatography. Melting points were determined by differential scanning calorimetry (DSC) using a Perkin Elmer DSC 7 instrument. LDI-TOF-MS were obtained using a Kratos Kompact Maldi 2 K-probe (Kratos Analytical) operating with pulsed extraction of the ions in linear high power mode. The samples were deposited directly onto a non-polished stainless steel sample plate from dichloromethane solution. ^{1}H and ^{13}C NMR spectra were recorded on a Bruker ARX 300 spectrometer (using the deuterated solvent as lock and tetramethylsilane as internal reference). Polarimetry was performed using a Dr. Kernchen Optik + ElectronikPropol polarimeter in a 1 cm cell.[25] Circular dichroism spectra were recorded on a JASCO-715 spectrometer. Magnetic susceptibility measurements were obtained with a Quantum Design SQUID magnetometer.

The EPR spectra were obtained using a Bruker ESP 300E spectrometer on solutions of radicals dissolved in 1 : 1 dichloromethane–toluene which were degassed with a flow of argon, according to a previously described method.[21] The hyperfine splitting parameters were obtained by simulation of spectra obtained in dilute solution. The intensity of the half field signal of the radicals was determined using the peak-picking method (which gave considerably less error than integration of the signals). During the recording of the spectra, special care was taken not to saturate the signal.

Preparation of (*R*)-methyl 2-(4-formylphenoxy)propionate ((*R*)-1). 4-Hydroxybenzaldehyde (400 mg, 3.28 mmol), (*S*)-methyl lactate (416 μL, 3.94 mmol) and triphenylphosphine (1.031 g, 3.94 mmol) were dissolved in dry THF (30 mL) with stirring under an atmosphere of argon, and the mixture was cooled in an ice bath. To this mixture, a solution of diethyl azodicarboxylate (DEAD, 685 μL, 3.94 mmol) in dry THF (5 mL) was added dropwise over a period of 30 minutes at 0 °C, and the mixture was allowed to warm up to room temperature with stirring overnight. After addition of water (10 mL), the THF was removed *in vacuo*, and the residue was partitioned between dichloromethane (50 mL) and water (50 mL), and the aqueous phase was extracted once more with the same solvent. The combined organic phases were dried over Na_2SO_4, filtered, and stripped of solvent. The residue was subject to column chromatography (SiO_2, hexane–CH_2Cl_2, 1 : 10), giving the product as a clear oil (581 mg, 82%). $[\alpha]_{546} = +46$ deg cm^2 g^{-1} ($c = 0.02$ M, in CH_2Cl_2); IR (neat): ν = 2995, 2957, 2846, 2740, 1757 (ν *C*(*O*)OCH$_3$), 1702 (ν *C*(*O*)H), 1592, 1484, 1451, 1260, 1136, 789 cm^{-1}; ^{1}H NMR (300 MHz, $CDCl_3$): $\delta = 1.67$ (d, $J = 6.9$ Hz, 3H, C*H*$_3$CH), 3.78 (s, 3H, OC*H*$_3$), 4.87 (q, $J = 6.9$ Hz, 1H, CH$_3$C*H*), 6.97 (d, $J = 8.6$ Hz, 2H, H-3 H-5), 7.83 (d, $J = 8.6$ Hz, 2H, H-2 H-6), 9.89 (s, 1H, C*H*O) ppm; ^{13}C NMR (75 MHz, $CDCl_3$); $\delta = 30.9$ (*C*H$_3$CH), 52.5 (O*C*H$_3$), 72.5 (CH$_3$*C*H), 115.1 (*C*3,*C*5), 130.6 (*C*1), 132.0 (*C*2,*C*6), 162.4 (*C*4), 171.4 (*C*OO), 190.7 (*C*HO) ppm.

Preparation of (*RS*)-methyl 2-(4-formylphenoxy)propionate ((*RS*)-1). The racemic compound was prepared in 70% yield

using the same procedure as that for the enantiomerically pure compound, employing (*RS*)-methyl lactate as the starting material, and gave identical analytical data with the exception that it presents no optical activity.

Preparation of (*R*)-methyl 2-[4-(4,5-dihydro-4,4,5,5-tetramethyl-3-oxido-1*H*-imidazol-3-ium-1-oxyl-2-yl)phenoxy]propionate ((*R*)-4MLNN). (*R*)-Methyl 2-(4-formylphenoxy)propionate ((*R*)-**1**, 144 mg, 0.69 mmol), 2,3-bis(hydroxylammonio)-2,3-dimethylbutane sulfate (**2**, 161 mg, 0.69 mmol) and $NaHCO_3$ (55 mg, 0.69 mmol) were combined in methanol (15 mL) and were stirred at room temperature for 24 hours. After the addition of aqueous $NaHCO_3$ (55 mg, 0.69 mmol in 15 mL), a precipitate formed. Without further purification, this solid was dissolved in CH_2Cl_2 (20 mL) and aqueous $NaIO_4$ (140 mg, 0.69 mmol in 10 mL) was added, and the mixture was stirred for 30 minutes at 0 °C. The organic phase was separated, and the aqueous phase was extracted further with CH_2Cl_2 (2 × 20 ml). The combined organic layers were dried over Na_2SO_4, filtered and stripped of solvent. The residue was subjected to column chromatography (SiO_2, AcOEt–CH_2Cl_2 1 : 12), giving the product as a blue amorphous solid (12%) Mp: 104 °C; UV–vis (CH_2Cl_2): λ_{max} (ε/L mol^{-1} cm^{-1}) = 280 (15000), 365 (10000), 618 nm (660); CD (CH_2Cl_2): λ_{max} ($\Delta\varepsilon$/L mol^{-1} cm^{-1}) = 270 (+1.2); IR (KBr): ν = 3444, 2987, 2945, 1757 (ν *C*(*O*)OCH$_3$), 1609, 1454, 1363 (ν NO), 1250, 1131, 835, 632, 540 cm^{-1}; LDI-TOF-MS: *m*/*z* = 335.3 ([M]$^+$) 321.2 [M − CH_2]$^+$; EPR (CH_2Cl_2–toluene 1 : 1): *g* factor, 2.0065; a_N, 7.65; a_{ortho}, 0.43; a_{meta}, 0.21; a_{Me}, 0.21.

Preparation of (*RS*)-methyl 2-[4-(4,5-dihydro-4,4,5,5-tetramethyl-3-oxido-1*H*-imidazol-3-ium-1-oxyl-2-yl)phenoxy]propionate ((*RS*)-4MLNN). Using the same procedure as for **(*R*)-4MLNN** but using (*RS*)-methyl lactate as starting material, the racemic modification was isolated as a blue solid in 30% yield. Mp 141 °C. Calculated for $C_{16}H_{21}O_5N_2$ (%) N 8.35, C 60.88, H 6.91. Found (%) 8.32, 60.77, 6.85; UV–vis (CH_2Cl_2): λ_{max} (ε/dm^3 mol^{-1} cm^{-1}) = 280 (15000), 365 (10000), 618 nm (660); IR (KBr): ν = 2988, 2960, 2929, 1754 (ν *C*(*O*)OCH$_3$), 1606, 1571, 1451, 1390, 1365 (ν *NO*), 1203, 1131, 1096, 841, 619, 542 cm^{-1}; LDI-TOF MS: *m*/*z* = 357.9 [M + Na]$^+$, 334.9 [M]$^+$, 320.9 [M − CH_2]$^+$, 305.0 [M − CH_2–O]$^+$; EPR (CH_2Cl_2–toluene 1 : 1): *g* factor, 2.0065; a_N, 7.67; a_{ortho}, 0.45; a_{meta}, 0.22; a_{Me}, 0.20.

Preparation of (*R*)-2-[4-(4,5-dihydro-4,4,5,5-tetramethyl-3-oxido-1*H*-imidazol-3-ium-1-oxyl-2-yl)phenoxy]propionic acid ((*R*)-4LNN). (*R*)-Methyl 2-[4-(4,5-dihydro-4,4,5,5-tetramethyl-3-oxido-1*H*-imidazol-3-ium-1-oxyl-2-yl)phenoxy]propionate ((*R*)-**4MLNN**, 100 mg, 0.3 mmol) was dissolved in a water (10 mL)–ethanol (10 mL) mixture with NaOH (1 g, 25 mmol) at ambient temperature and the mixture was stirred for 3 h. After acidifying with HCl (aq, 10%), the product was extracted with CH_2Cl_2 (3 × 20 mL). The combined organic layers were dried over Na_2SO_4, filtered and stripped of solvent. The residue was crystallised from CH_2Cl_2–hexane as dark blue needles (97%). Mp 152 °C. Calculated for $C_{16}H_{21}O_5N_2$ (%) N 8.72, C 59.80, H 6.59. Found (%) 8.37, 59.14, 6.42; UV–vis (CH_2Cl_2): λ_{max} (ε/dm^3 mol^{-1} cm^{-1}) = 281 (15000), 367 (10000), 617 nm (620); CD (CH_2Cl_2): λ_{max} ($\Delta\varepsilon$) = 290 (−0.69); IR (KBr): ν = 3440, 2984, 2503 (ν C(O)*OH*), 1741(ν *C*(*O*)OH), 1604, 1488, 1346 (ν NO), 1298, 1256, 1134, 1087, 833 cm^{-1}; LDI-TOF MS: *m*/*z* = 360.0 [M + K]$^+$, 344.0 [M + Na]$^+$, 329.0 [M + Li]$^+$, 321.0 [M]$^+$, 307.1 [M − CH_2]$^+$, 291.0 [M − CH_2–O]$^+$; EPR (CH_2Cl_2–toluene 1 : 1): *g* factor, 2.0065; a_N, 7.67; a_{ortho}, 0.46; a_{meta}, 0.20; a_{Me}, 0.20.

Preparation of (*RS*)-2-[4-(4,5-dihydro-4,4,5,5-tetramethyl-3-oxido-1*H*-imidazol-3-ium-1-oxyl-2-yl)phenoxy]propionic acid ((*RS*)-4LNN). Using the same procedure as for **(*R*)-4LNN** but using (*RS*)-methyl 2-[4-(4,5-dihydro-4,4,5,5-tetramethyl-3-oxido-1*H*-imidazol-3-ium-1-oxyl-2-yl)phenoxy]propionate ((*RS*)-**4MLNN**) as starting material, the racemic modification was isolated as a blue solid in 94% yield. Mp: 145 °C. Calculated for $C_{16}H_{21}O_5N_2$ (%) N 8.72, C 59.80, H 6.59. Found (%) 8.32, 59.23, 6.40; UV–vis (CH_2Cl_2): λ_{max} (ε/dm^3 mol^{-1} cm^{-1}) = 281 (14000), 365 (9300), 618 nm (600); LDI-TOF MS: *m*/*z* = 360.0 [M + K]$^+$, 344.0 [M + Na]$^+$, 329.0 [M + Li]$^+$, 321.0 [M]$^+$, 307.1 [M − CH_2]$^+$; EPR (CH_2Cl_2 : toluene 1 : 1): *g* factor, 2.0065; a_N, 7.67; a_{ortho}, 0.50; a_{meta}, 0.21; a_{Me}, 0.19.

X-Ray diffraction analyses

The X-ray crystal structures were solved by direct methods using SHELXS-86[26] and refined with anisotropic displacement parameters by using SHELXL-97.[27] Diffractometer Bruker P4, Scan type ω. Of the hydrogen atoms, only those of the hydroxy groups of (*R*)-**4LNN** and (*RS*)-**4LNN** were refined as regular atoms. The data have been deposited with the Cambridge Crystallographic Data Centre. CCDC reference numbers 170508–170510. See http://www.rsc.org/suppdata/jm/b1/b106239p/ for crystallographic files in .cif or other electronic format.

Acknowledgement

This work was supported by grants from the DGES, Spain (Proyecto n° MAT2000-1388-C03-01), the 3MD Network of the TMR program of the EU (Contract ERBFMRXCT 980181), an Acción Integrada Hispano-Austriaco (HU1999-0015), and the Fundación Ramón Areces. M. M. thanks the Fundación Ramón Areces for a PhD fellowship.

References

1 For general reviews of stereochemistry, see: (*a*) E. L. Eliel and S. H. Wilen, *Stereochemistry of Organic Compounds*, J. Wiley & Sons, New York, 1994; (*b*) A. N. Collins, G. N. Sheldrake and J. Crosby, *Chirality in Industry Vols. I and II*, J. Wiley & Sons, New York, 1992 and 1997; (*c*) *Supramolecular Stereochemistry*, ed. J. Siegel, NATO ASI Series C 473, Kluwer, Dordrecht, 1995.

2 For reviews of the influences of chirality in materials, see: (*a*) J. W. Goodby, *J. Mater. Chem.*, 1991, **1**, 307–318; (*b*) G. Solladie and R. G. Zimmermann, *Angew. Chem., Int. Ed. Engl.*, 1994, **23**, 348–362; (*c*) T. J. Marks and M. A. Ratner, *Angew. Chem., Int. Ed. Engl.*, 1995, **34**, 155–173.

3 (*a*) V. A. Markelov, M. A. Novikov and A. A. Turkin, *JETP Lett. Engl. Transl.*, 1977, **25**, 378; (*b*) G. L. J. A. Rikken and E. Raupach, *Nature*, 1997, **390**, 493–494; (*c*) G. L. J. A. Rikken and E. Raupach, *Phys. Rev. E*, 1998, **58**, 5081–5084; (*d*) P. Kleindienst and G. H. Wagnière, *Chem. Phys. Lett.*, 1998, **288**, 89–97.

4 (*a*) A. Caneschi, D. Gatteschi, P. Rey and R. Sessoli, *Inorg. Chem.*, 1991, **30**, 3936–3941; (*b*) S. Decurtins, H. W. Schmalle, R. Pellaux, R. Huber, P. Fischer and B. Ouladdiaf, *Adv. Mater.*, 1996, **8**, 647–651; (*c*) P. Day in *Supramolecular Engineering of Synthetic Metallic Materials: Conductors and Magnets*, eds. J. Veciana, C. Rovira and D. B. Amabilino, NATO ASI Series C518, Kluwer, Dordrecht, 1998, pp. 253–269; (*d*) K. Nakayama, T. Ishida, R. Takayama, D. Hashizume, M. Yasui, F. Iwasaki and T. Nogami, *Chem. Lett.*, 1998, 497–498; (*e*) Y. Zhang, S. Wang, G. D. Enright and S. R. Breeze, *J. Am. Chem. Soc.*, 1998, **120**, 9398–9399; (*f*) R. Andrés, M. Gruselle, B. Malézieux, M. Verdaguer and J. Vaissermann, *Inorg. Chem.*, 1999, **38**, 4637–4646; (*g*) P. Day, *Coord. Chem. Rev.*, 1999, **190–192**, 827–839; (*h*) S. Decurtins, *Philos. Trans. R. Soc. London A*, 1999, **357**, 3025–3040; (*i*) H. Kumagai and K. Inoue, *Angew. Chem., Int. Ed.*, 1999, **38**, 1601–1603.

5 (*a*) R. W. Kreilick, J. Becher and E. F. Ullman, *J. Am. Chem. Soc.*, 1969, **91**, 5121–5124; (*b*) R. J. Weinkman and E. C. Jorgensen, *J. Am. Chem. Soc.*, 1971, **93**, 7028–7033; (*c*) R. J. Weinkman and E. C. Jorgensen, *J. Am. Chem. Soc.*, 1971, **93**, 7033–7038; (*d*) K. Scheffler, U. Höfler, P. Schuler and H. B. Stegmann, *Mol. Phys.*, 1988, **65**, 439–446; (*e*) M. Mäurer, K. Scheffler, H. B. Stegmann and A. Mannschreck, *Angew. Chem., Int. Ed. Engl.*, 1991, **30**, 602–604; (*f*) E. Joerss, P. Schuler, C. Maichle-Moessmer, S. Abram and H. B. Stegmann, *Enantiomer*, 1997, **2**, 5–16; (*g*) P. Schuler, F. M. Schaber, H. B. Stegmann

and E. Janzen, *Magn. Reson. Chem.*, 1999, **37**, 805–813; (*h*) R. Tamura, S. Susuki, N. Azuma, A. Matsumoto, F. Toda, A. Kamimura and K. Hori, *Angew. Chem., Int. Ed. Engl.*, 1994, **33**, 878–879R. Tamura, S. Susuki, N. Azuma, A. Matsumoto, F. Toda, T. Takui, D. Shiomi and K. Itoh, *Mol. Cryst. Liq. Cryst.*, 1995, **271**, 91–96S. D. Rychnovsky, T. L. McLernon and H. Rajapakse, *J. Org. Chem.*, 1996, **61**, 1194–1195Y. Ishino, T. Ikeda, A. Kajiwara, Y. Morishimo, W. Mori, K. Yamaguchi, Y. Miyako and M. Kamachi, *Mol. Cryst. Liq. Cryst.*, 1997, **305**, 41–54J-P. Sutter, S. Golhen, L. Ouahab and O. Kahn, *C. R. Acad. Sci., Sér. IIc: Chim.*, 1998, 63–68J. Sedó, N. Ventosa, D. Ruiz-Molina, M. Mas, E. Molins, C. Rovira and J. Veciana, *Angew. Chem., Int. Ed.*, 1998, **37**, 330–333.

6 (*a*) M. Minguet, D. B. Amabilino, I. Mata, E. Molins and J. Veciana, *Synth. Met.*, 1999, **103**, 2253–2256; (*b*) M. Minguet, D. B. Amabilino, J. Cirujeda, K. Wurst, I. Mata, E. Molins, J. J. Novoa and J. Veciana, *Chem. Eur. J.*, 2000, **6**, 2350–2361; (*c*) M. Minguet, D. B. Amabilino, K. Wurst and J. Veciana, *Monatsh. Chem.*, 2001, **132**, 71–82; (*d*) M. Minguet, D. B. Amabilino, K. Wurst and J. Veciana, *J. Chem. Soc., Perkin Trans. 2*, 2001, 670–676.

7 For reviews, see: (*a*) S. Nakatsuji and H. Anzai, *J. Mater. Chem.*, 1997, **7**, 2161–2174; (*b*) *Magnetic Properties of Organic Materials*, ed. P. M. Lathi, Marcel Dekker, New York, 1999; (*c*) D. B. Amabilino and J. Veciana, in *Magnetism–Molecules to Materials Volume II: Molecule Based Materials*, eds. J. S. Miller and M. Drillon, Wiley-VCH, Weinheim, 2001. For recent examples, see:; (*d*) J.-P. Sutter, N. Daro, S. Golhen, L. Ouahab and O. Kahn, *Mol. Cryst. Liq. Cryst.*, 1999, **334**, 69–79; (*e*) N. Yoshioka, N. Matsuoka, M. Irisawa, S. Ohba and H. Inoue, *Mol. Cryst. Liq. Cryst.*, 1999, **334**, 239–246; (*f*) Y. Pontillon, T. Akita, A. Grand, K. Kobayashi, E. Lelievre-Berna, J. Pécaut, E. Ressouche and J. Schweizer, *J. Am. Chem. Soc.*, 1999, **121**, 10126–10133; (*g*) F. M. Romero, R. Ziessel, M. Bonnet, Y. Pontillon, E. Ressouche, J. Schweizer, B. Delley, A. Grand and C. Paulsen, *J. Am. Chem. Soc.*, 2000, **122**, 1298–1309.

8 O. Kahn, *Molecular Magnetism*, VCH, Weinheim, 1993.

9 (*a*) O. Mitsunobu, *Synthesis*, 1981, 1–25; (*b*) D. L. Hughes, *Org. React. (N.Y.)*, 1992, **42**, 335–656.

10 (*a*) M. Lamchen and T. W. Mittag, *J. Chem. Soc.*, 1966, **C**, 2300–2303; (*b*) V. Ovcharenko and S. Fokin, *P. Rey, Mol. Cryst. Liq. Cryst.*, 1999, **334**, 109–119.

11 E. F. Ullman, J. H. Osiecki, D. G. B. Boocock and R. Darcy, *J. Am. Chem. Soc.*, 1972, **94**, 7049–7059.

12 D. B. Amabilino, J. Cirujeda and J. Veciana, *Philos. Trans. R. Soc. London A*, 1999, **357**, 2873–2891.

13 (*a*) R. Taylor and O. Kennard, *J. Am. Chem. Soc.*, 1982, **104**, 5063–5070; (*b*) G. R. Desiraju, *Acc. Chem. Res.*, 1996, **29**, 441–449; (*c*) T. Steiner, *Chem. Commun.*, 1997, 727–734; (*d*) T. Steiner, *Chem. Commun.*, 1999, 313–314; (*e*) G. Mehta, R. Vidya and K. Venkatesan, *Tetrahedron Lett.*, 1999, **40**, 2417–2420; (*f*) S. S. Kuduva, D. C. Craig, A. Nangia and G. R. Desiraju, *J. Am. Chem. Soc.*, 1999, **121**, 1936–1944; (*g*) Y. Gu, T. Kar and S. Scheiner, *J. Am. Chem. Soc.*, 1999, **121**, 9411–9422; (*h*) G. R. Desiraju and T. Steiner, *The Weak Hydrogen Bond in Structural Chemistry and Biology*, Oxford University Press, Oxford, 1999.

14 This type of hydrogen bond is relatively common in this family of radicals and are thought to participate in the propagation of magnetic interactions. See, for example: (*a*) J. Cirujeda, M. Mas, E. Molins, F. Lanfranc de Panthou, J. Laugier, J. G. Park, C. Paulsen, P. Rey, C. Rovira and J. Veciana, *J. Chem. Soc., Chem. Commun.*, 1995, 709–710; (*b*) E. Hernández-Gasio, M. Mas, E. Molins, C. Rovira and J. Veciana, *Angew. Chem., Int. Ed. Engl.*, 1993, **32**, 882–884; (*c*) O. Jürgens, J. Cirujeda, M. Mas, I. Mata, A. Cabrero, J. Vidal-Gancedo, C. Rovira, E. Molins and J. Veciana, *J. Mater. Chem.*, 1997, **7**, 1723–1730; (*d*) J. J. Novoa, M. Deumal, M. Kinoshita, Y. Hosokishi, J. Veciana and J. Cirujeda, *Mol. Cryst. Liq. Cryst.*, 1997, **305**, 129–141; (*e*) S. Nakatsuji, M. Saiga, N. Haga, A. Naito, M. Nagakawa, Y. Oda, K. Suzuki, T. Enoki and H. Anzai, *Mol. Cryst. Liq. Cryst.*, 1997, **306**, 279–284; (*f*) J. J. Novoa and M. Deumal, *Mol. Cryst. Liq. Cryst.*, 1997, **305**, 143–156; (*g*) S. Nakatsuji, M. Saiga, N. Haga, A. Naito, T. Hirayama, M. Nakagawa, Y. Oda, H. Anzai, K. Suzuki, T. Enoki, M. Mito and K. Takeda, *New J. Chem.*, 1998, **22**, 275–280; (*h*) O. Jürgens, J. Vidal-Gancedo, C. Rovira, K. Wurst, C. Sporer, B. Bildstein, H. Schottenberger, P. Jaitner and J. Veciana, *Inorg. Chem.*, 1998, **37**, 4547–4558; (*i*) J. J. Novoa, M. Deumal and J. Veciana, *Synth. Met.*, 1999, **103**, 2283–2286.

15 M. Minguet, D. B. Amabilino, J. Vidal-Gancedo, K. Wurst and J. Veciana, *Mol. Cryst. Liq. Cryst.*, 1999, **334**, 347–358.

16 (*a*) O. Wallach, *Liebigs Ann. Chem.*, 1895, **286**, 90–143; (*b*) for a recent critical appraisal of the rule see: C. Pratt-Brock, W. B. Schweizer and J. D. Dunitz, *J. Am. Chem. Soc.*, 1991, **113**, 9811–9820.

17 J. Orduna, J. Garín, C. Boulle, J. Cirujeda, O. Jürgens and J. Veciana, *Rapid Comun. Mass Spectrom.*, 1997, **11**, 1103–1106.

18 (*a*) C. Moucheron, C. O. Dietrich-Buchecker, J.-P. Sauvage and A. van Dorsselaer, *J. Chem. Soc. Dalton Trans.*, 1994, 885–893; (*b*) K. C. Russell, E. Leize, A. van Dorsselaer and J.-M. Lehn, *Angew. Chem., Int. Ed.*, 1995, **34**, 209–213; (*c*) X. Cheng, Q. Gao, R. D. Smith, E. E. Simanek, M. Mammen and G. M. Whitesides, *J. Org. Chem.*, 1996, **61**, 2204–2206; (*d*) M. Przybylski and M. O. Glocker, *Angew. Chem., Int. Ed.*, 1996, **35**, 806–826; (*e*) F. M. Romero, R. Ziessel, A. Dupont-Gervais and A. Von Dorsselaer, *Chem. Commun.*, 1996, 551–553; (*f*) K. Tashiro, T. Aida, J.-Y. Zheng, K. Kinbara, K. Saigo, S. Sakamoto and K. Yamaguchi, *J. Am. Chem. Soc.*, 1999, **121**, 9477–9478; (*g*) R. Sussmuth, G. Jung, F. J. Winkler and R. Medina, *Eur. Mass Spectrom.*, 1999, **5**, 289–294; (*h*) F. Hof, C. Nuckolls and J. Rebek Jr., *J. Am. Chem. Soc.*, 2000, **122**, 4251–4252.

19 (*a*) M. Sheves, B. Kohne, N. Friedman and Y. Mazur, *J. Am. Chem. Soc.*, 1984, **106**, 5000–5002; (*b*) K. Kobayashi, Y. Asakawa, Y. Kikuchi, H. Toi and Y. Aoyama, *J. Am. Chem. Soc.*, 1993, **115**, 2648–2654; (*c*) J. E. Forman, R. E. Barrans Jr. and D. A. Dougherty, *J. Am. Chem. Soc.*, 1995, **117**, 9213–9228; (*d*) M. Kodaka, *J. Phys. Chem. A*, 1998, **102**, 8101–8103; (*e*) H.-Y. Liu, J.-W. Huang, X. Tian, X.-D. Jiao, G.-T. Luo and L.-N. Ji, *Inorg. Chim. Acta*, 1998, **272**, 295–299; (*f*) M. Asakawa, P. R. Ashton, W. Hayes, H. K. Janssen, E. W. Meijer, S. Menzer, D. Pasini, J. F. Stoddart, A. J. P. White and D. J. Williams, *J. Am. Chem. Soc.*, 1998, **120**, 920–931; (*g*) S. Hamai and T. Koshiyama, *J. Photochem. Photobiol., A*, 1999, **127**, 135–141; (*h*) S. Yagi, H. Kitayama and T. Takagishi, *J. Chem. Soc., Perkin Trans 1*, 2000, 925–932.

20 In the compounds related to (*R*)-**3LNN**, a significant Cotton effect is seen in the visible region in solution (see ref. 6*b*). This situation might be favoured by the formation of intramolecular hydrogen bonds which have been observed in the solid state for (*R*)-**3MLNN** (see ref 6*d*) which draw near the nitroxide moiety to the stereogenic centre.

21 J. Cirujeda, J. Vidal-Gancedo, O. Jürgens, F. Mota, J. J. Novoa, C. Rovira and J. Veciana, *J. Am. Chem. Soc.*, 2000, **122**, 11393–11405.

22 The SOMO in these radicals is located on the ONCNO unit, with a node located on the central carbon atom. For discussions, see: (*a*) A. Zheludev, E. Ressouche, J. Schweizer, P. Turek, M. Wan and H. Wang, *Solid State Commun.*, 1994, **90**, 233–235; (*b*) A. Zheludev, M. Bonnet, E. Ressouche, J. Schweizer, M. Wan and H. Wang, *J. Magn. Magn. Mater.*, 1994, **135**, 147–160; (*c*) Y. Pontillon, A. Caneschi, D. Gatteschi, A. Grand, E. Ressouche, R. Sessoli and J. Schweizer, *Chem. Eur. J.*, 1999, **5**, 3616–3624; (*d*) B. Gillon, M. A. Aebersold, O. Kahn, L. Pardi and B. Delley, *Chem. Phys.*, 1999, **250**, 23–34; (*e*) S. Pillet, M. Souhassou, Y. Pontillon, A. Caneschi, D. G2tteschi and C. Leconte, *New J. Chem.*, 2001, **25**, 131–143, and ref. 21.

23 See, for example: (*a*) Y.-S. Chen, J. W. Kampf and R. G. Lawton, *Tetrahedron Lett.*, 1997, **38**, 5781–5784; (*b*) R. Atencio, L. Brammer, S. Fang and F. C. Pigge, *New J. Chem.*, 1999, **23**, 461–463; (*c*) I. Pálinkó, *Acta Crystallogr., Sect. B*, 1999, **55**, 216–220 . It is interesting to note that a lactic acid derivative, 2-(4-chlorophenoxy)propionic acid, crystallises to form dimers in the racemate; (*d*) C. H. L. Kennard, G. Smith and A. H. White, *Acta Crystallogr., Sect. B*, 1982, **38**, 868–875; (*e*) S. Raghunathan, K. Chandrasekhar and V. Pattabi, *Acta Crystallogr., Sect. B*, 1982, **38**, 2536–2538 , while the enantiopure compound crystallises as a chain; (*f*) H. O. Sørensen, A. Collet and S. Larsen, *Acta Crystallogr., Sect. C*, 1999, **55**, 953–956.

24 In the structures reported so far of nitronyl nitroxide derivatives bearing carboxylic acid functionalities, the acidic hydrogen atom participates in a hydrogen bond with the nitrone: (*a*) K. Inoue and H. Iwamura, *Chem. Phys. Lett.*, 1993, **305**, 367–384; (*b*) C. Bätz, P. Amman, H. J. Deriseroth and L. Dulog, *Liebigs Ann. Chem.*, 1994, 739–740; (*c*) O. Félix, M. W. Hosseini, A. D. Cian, J. Fischer, L. Catala and P. Turek, *Tetrahedron Lett.*, 1999, **40**, 2943–2946; (*d*) C. Stroh, F. M. Romero, N. Kyritsakas, L. Catala, P. Turek and R. Ziessel, *J. Mater. Chem.*, 1999, **9**, 875–882.

25 Polarimetry of the nitronyl nitroxide radicals reported here was not possible on account of the high optical absorption : optical rotatory power ratio that these compounds possess.

26 G. M. Sheldrick, University of Göttingen, Germany, 1990.

27 G. M. Sheldrick, University of Göttingen, Germany, 1997.